3D discrete kinematic modelling applied extensional and compressional tectonic

T. CORNU[1], F. SCHNEIDER[1] & J.-P. GRATIER[2]

[1]*IFP, 1–4 avenue de Bois-Préau, 92500 Rueil-Malmaison, France (e-mail tristan.cornu@ifp.fr; frederic.schneider@ifp.fr)*

Present address: Faculty of Earth and Life Sciences, Tectonics, Vrije Universit Boelelaan 1085, 1081 HV Amsterdam, The Netherlands (e-mail: tristan.cornu@fa

[2]*LGIT, Observatoire de l'Université de Grenoble, IRIGM, BP 53, 38041 Grenobl (e-mail: Jean-Pierre.Gratier@obs.ujf-grenoble.fr)*

Abstract: The 3D simulation of coupled backward and forward deformation of geological laye is a new step in basin modelling. Although this problem could be addressed with either mecha ical or kinematic approaches, the mechanical approach remains too complex to be address properly. The kinematic model described here allows a geologically valid path, which takes int account an incremental evolution in time. To obtain a better description of 3D geometries, th model uses a full hexaedric discretization and the discrete neutral surface of each layer is use when performing the flexural slip deformation. An application to a synthetic geological case then proposed, to study the behaviour of the structure in compressional and extensional context

Modelling the evolution and petroleum potential of sedimentary basins is a complex problem, involving two distinct steps: (1) the simulation of the tectonic deformation, and (2) the computation of the hydrocarbon generation and migration. Until now, most basin modelling tools were constructed to address only one of these problems (Schneider & Wolf in press; Zoetmeyer 1992). A first attempt to couple deformation and fluid flow simulations was done recently (Schneider *et al.* 2000) but it is still limited to 2D cases with relatively simple kinematic patterns (vertical shear mechanism). The model we propose here is a discrete model for 3D flexural slip deformation (or mixed flexural slip and vertical shear), where further computations to solve fluid flow simulations might be done by using the mesh of the deformed elements.

Two distinct approaches can be chosen to model the tectonic deformations that occur in a sedimentary basin: (1) a mechanical approach, or (2) a kinematic approach. The mechanical approach has already been tested on analytical or geological cases (Barnichon 1998; Niño *et al.* 1998; Erickson and Jamison 1995; Bourgeois 1997; Coussy 1995). However, these studies were done on 2D cases with simplified assumptions on the mechanical behaviour of the rocks. 3D mechanical modelling that would include all the parameters relevant to natural deformation has never yet been proposed. This may be explained by the extreme of the mathematical formulation and limitations on one hand, and on the oth the complexity of the phenomenon at time and space scales (Ramsay & Hu which makes it difficult to find the ada ogical laws and boundary conditions. Ev like 3DEC (Cundall 1988; Hart *et al.* 1 ited by its restrictive hypothesis of i deformation within deformed blocks, w realistic for natural deformation of s basins.

To overcome the difficulty of the approach, geologists have instead focu kinematic approach (Dahlstrom 1969), w geometrical translation of mechanical as Kinematic modelling is a good alterna can be sufficiently representative of the r cesses. A discrete approach (Waltham 1 Diviès 1997) can also be used for furt tation of thermal and fluid transfers, int rock attributes (i.e. porosity, permeabili conductivity, etc.), and simulation of n cesses (i.e. sedimentation, eros compaction). One limitation of the exist atic approaches is that the proposed m either to forward modelling (Suppe 1 1983; De Paor 1988*a*, *b*; Contreras and S or to backward restoration (Moretti 19

From: NIEUWLAND, D. A. (ed.) *New Insights into Structural Interpretation and Modelling*. Geological S

et al. 1991; Gratier & Guillier 1993; Bennis *et al.* 1991). Therefore the modelling of tectonic deformation relies on two types of models to solve the problem of restoration and deformation (Egan *et al.* 1998). However, the main limitation is that most of the kinematic models are 2D, or 'pseudo-3D' at best (Wilkerson & Medwedeff 1991; Shaw *et al.* 1994). These pseudo-3D models extend the area conservation to volume conservation, but are limited to cylindrical cases, built with topologically equivalent 2D sections. The main restriction is that the associated finite displacement must be parallel in map view. To overcome these problems, we have developed and present here a discrete algorithm that can be used both for backward and forward modelling, and that can be applied to real 3D cases. The method is applied to an analytical sedimentary basin with a lateral termination, derived from real field structures.

The model

The assumptions used to describe the 3D flexural slip mechanism are first briefly presented. The model is supported by three main assumptions.

(1) Each layer of the basin is assumed to be independent, and the sliding between the layers is supposed to be perfect.
(2) As a general simplification, we assume that the thickness of the layer is preserved through the whole progressive deformation. Alternatively, thickness changes could be integrated if required.
(3) Because the flexural-slip mechanism would preserve the length of the neutral line of a layer, we assume that the area of the neutral surface is also kept constant in 3D.

Layer slip and preservation of the layer thickness are the most commonly used assumptions in literature (Suppe 1983; Waltham 1989, 1990), and they are consistent with the geological observations of the deformation of so-called competent layers (Ramsay & Huber 1987). The last assumption is a mechanical one, as it relies on the flexural-slip mechanism and deals with the neutral surface of a layer, which is supposed to conserve its area through deformation (Ramsay & Huber 1987). This is a powerful and useful assumption since further calculation of the progressive deformation will be greatly simplified by the use of a surface instead of a volume.

We take a discrete modelling approach here, and implementation of the algorithm is done in C++. The geological objects are defined as follows.

1. The basin defines the entire geological area. It contains all the tectonic portion of the studied domain within its geometric boundaries.
2. The faults are defined as the m discontinuity within the domain the subdivision of the basin in number of subdomains, and the as triangulated surfaces.
3. Each subdomain of the basin c independent block, which is bor faults (footwall, hanging-wall). T are defined either by a fault or by of the basin.
4. The layers are the simplified g resentation of the lithologic be discretized with hexaedric eleme vertices, and they support the algorithm.

Mathematical description

The first step of the modelling is to all the layers of each block are elements. The elements are he hexaedric element, with six faces always coplanar. After the definitio logical domains, the motion of the elled through the displacement of ea neutral surface of the layers. The neu defined here as the median surface c passes through the middle point of edges of each hexaedric element (Fi

Sliding support

The support of sliding is defined wit element in each layer. For the firs block, we use the base faces of the el upper layer we use the roof faces o layer, and for the lateral surface of s the faces that coincide with the latera der. Each face is defined by four ve cut them into two triangles of three allows us to define the surface of s piecewise surface, or plane:

$$(P): \alpha x + \beta y + \gamma z + h = 0$$

where α, β, γ, h are defined with t of the three vertices.

Bisector plane

The bisector planes define the inter planes, and they will help us to pr tance through the displacement. Th with the help of the coordinates of they cut.

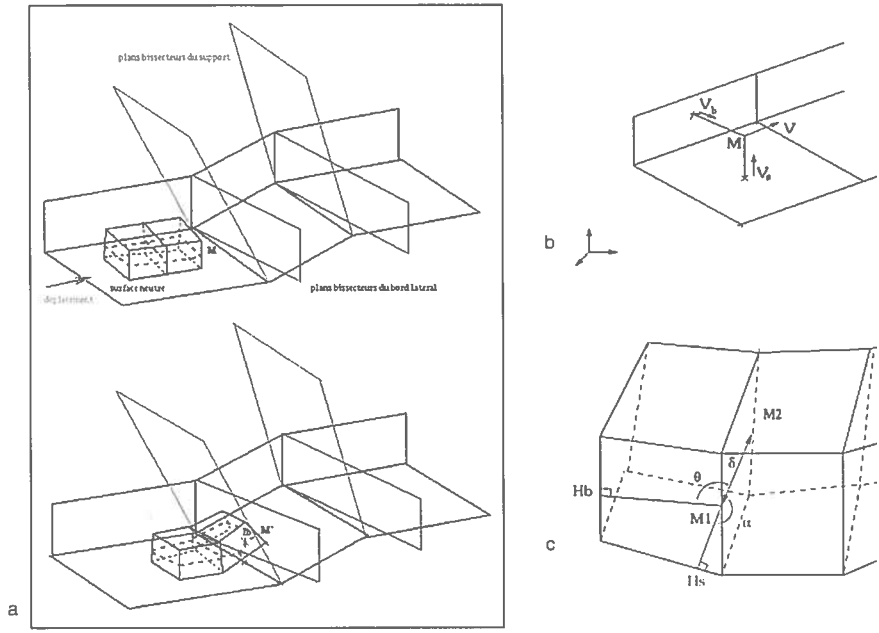

Fig. 1. (**a**) Diagram of the deformation of a layer with the algorithm based on neutral surface conservatic of the construction of the displacement direction for the bottom layer; (**c**) diagram of the construction ‹ ment direction for the upper layers.

Curvilinear displacement

The movement of a neutral surface point is achieved with a curvilinear displacement $\vec{t}_{\delta}\vec{v}$, where δ is the distance of displacement, and $\vec{v}$ the direction of displacement. Due to the third space component, the direction of the displacement will depend not only on the basement, but also on the lateral border. We define $\vec{v}$ as:

$$\vec{v} = \vec{n}_s \wedge \vec{n}_b$$

where $\vec{n}_s$ is the normal vector of the support on which the layer slips, and $\vec{n}_b$ the normal vector of an imposed lateral surface (Fig. 1b).

The definition of $\vec{v}$ imposes to the displacement to be parallel both to the support and to the imposed lateral border. This first approximation provides a conservation of the width of the layer (the distance between each point of the neutral surfaces and the lateral boundary).

Displacement step of a neutral surface node

$M_0(x_0, y_{0,0})$ is a node of the neutral surface. It is displaced following the draw $D(M, \vec{v})$:

$$D: \begin{cases} x_0 + \mathrm{v}_x t \\ y_0 + \mathrm{v}_y t \\ z_0 + \mathrm{v}_z t \end{cases}$$

The point M_0 follows (D) until it inte bisector plane that split the domai bisector plane of the basement, (P_{Bb}) plane of the lateral imposed border, ‹

$$(P_{Bs}): \alpha_{bs}\, x + \beta_{bs}\, y + \gamma_{bs}\, z + h_{bs} =$$

$$(P_{Bb}): \alpha_{bb}\, x + \beta_{bb}\, y + \gamma_{bb}\, z + h_{bb} =$$

The coordinates of $I_i = (D) \cap (P_{Bi}, i$ section point of (D) and the bisectc are written:

$$I_i = \begin{cases} x_0 + \mathrm{v}_x t_{Ii} \\ y_0 + \mathrm{v}_y t_{Ii} \\ z_0 + \mathrm{v}_z t_{Ii} \end{cases}$$

The position of M_0 relative to the b is not known a priori, so we are oblige the two intersection points, with ‹ definition of t_{Ii}:

$$t_{Ii} = \frac{-(\alpha_{bi}x_0 + \beta_{bi}y_0 + \gamma_{bi}z_0 + h_{bi})}{\alpha_{bi}v_x + \beta_{bi}v_y + \gamma_{bi}v_z}$$

We suppose $d_i = \|MI_i\|$ to be the Euclidean distance between the two points I_i and M. The point M has to displace an amount of δ. Before the displacement, we must define which bisector plane is first cut by (D). It will be nearest the one with the smallest distance d_i. When the plane is determined, we have three cases:

(1) $d_i > \delta$: the point M has a displacement of δ along (D), and its new coordinates are:

$$M = \begin{cases} x_0 + v_x\delta \\ y_0 + v_y\delta \\ z_0 + v_z\delta \end{cases}$$

(2) $d_i = \delta$: the point M is the same than point I_i.
(3) $d_i < \delta$: M is displaced to I_i, but it still must displace a distance $\delta - d_i$. We repeat all the precedent operations, with initial point I_i and a new definition of $\vec{v}$ according to the basement and the lateral border.

Reconstruction of upper layers

The reconstruction of the upper layers tries to rebuild a geometry which conserves the angular and distance relationships of the previous step configuration. The complexity of the reconstruction comes from the parameters we have to define: the distance δ between two nodes of the neutral surface, and two angles α and θ relative to the basement and to the lateral border (Fig. 1c).

M_1 and M_2 are two successive points of the neutral surface: $\delta = \|M_1M_2\|$. H_s and H_b are the normal projection of M_1 upon the basement and upon the lateral imposed border:

$$\cos\alpha = \frac{\overrightarrow{M_1M_2}.\overrightarrow{M_1H_s}}{\|\overrightarrow{M_1M_2}.\overrightarrow{M_1H_s}\|}$$

$$\cos\theta = \frac{\overrightarrow{M_1M_2}.\overrightarrow{M_1H_b}}{\|\overrightarrow{M_1M_2}.\overrightarrow{M_1H_b}\|}$$

The direction of displacement $\vec{v}$ must now be defined according to α and θ. To do this, we place ourselves in a reference system $\Re(M_1, \vec{e}_1, \vec{e}_2, \vec{e}_3)$, where:

$$\vec{e}_1 = \frac{\overrightarrow{M_1H_s}}{\|\overrightarrow{M_1H_s}\|}$$

$$\vec{e}_2 = \frac{\overrightarrow{M_1H_b}}{\|\overrightarrow{M_1H_b}\|}$$

$$\vec{e}_3 = \frac{\overrightarrow{M_1H_s} \wedge \overrightarrow{M_1H_b}}{\|\overrightarrow{M_1H_s} \wedge \overrightarrow{M_1H_b}\|}$$

We can define v as:

$$\vec{v} = a\vec{e}_1 + b\vec{e}_2 + c\vec{e}_3$$

with:

$$\vec{v}.\vec{e}_1 = \cos\alpha$$
$$\vec{v}.\vec{e}_2 = \cos\theta$$
$$\|\vec{v}\| = 1 = \sqrt{a^2 + b^2 + c^2}$$

Volume reconstruction

After the displacement of all the node: tral surface of a layer, we have to res ume of the layer. To perform this res use the vertical edges. Each node of surface belongs by definition to a v Thus, after displacement, we rebuilt th a rigid rotation of the vertical edge.

Geological application

The test was done on a synthetic ca structed a geometric model (Fig. 2), w lar to a field area in the Gulf of Mexi *et al.* 1999, fig. 2c; Rowan *et al.* 19 or to Niger Delta structures (Crans However, we are not trying to make these areas, which are only named to h what kind of application could be ex the model. Such a structure contains sional and compressional structures, from gravity sliding processes. We ass servation of the global volume of t (contained between the two main fa such a deformation. We also impose mination of the structure in order to r eral 3D evolution both in space and way, we can study the evolution of a p mentary basin ending along a non-ve ramp. With this experiment, we hope mation on the 3D behaviour of the st it is subjected to gravity sliding. We w the local volume variations and the lateral ramp on the displacement field

The limits (Fig. 2c) of the footwal by a normal fault with a 20° dip a reverse fault with a 20° dip at the fro eral ramp with a 70° dip along one la ary. The other lateral boundary is free. wall is a block of 11286 elements. T sequence is made up of a composite eleven layers of various thicknesses behaviour of the algorithm with dif nesses. The length of the model is width is 10000 m, and its thickness is

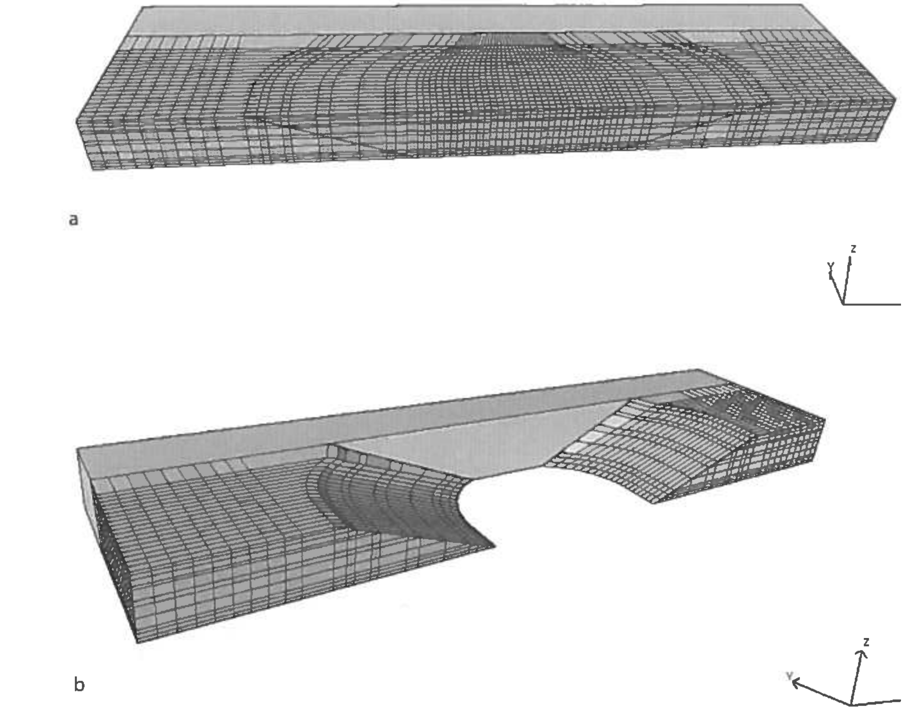

Fig. 2. (**a**) basin at the initial state; (**b**) description of the domain boundaries.

2b). The kinematic boundary condition is applied at the back of the hanging wall and imposes a displacement of 1000 m in the x direction at each time step. This means that all the elements of the first layer will move of 1000 m, and that those of the upper layers will be reconstructed according to the first layer deformation. All layers are supposed to deform by flexural slip, although it could also be possible to integrate other deformation mechanisms such as vertical shear for some layers. The footwall is supposed to be rigid, and is also discretized because its top helps to define the sliding support.

In Figure 3a–e we illustrate the evolution of the basin after four time steps and thus 4000 m of displacement. Below, we will outline our major observations.

Basin geometry

The resulting geometry remains consistent with the initial shape, and displays no anomalous or unexpected deformations like crossing edges. The global volume variation of the hanging wall after deformation is lower than 1% or 2%. This is an acceptable and realistic result. It implies that even if the volume conservation was not an independent constraint, the coupled assumptions made on the neutral surface and on the edge rebuild evant.

Transport direction

In Figure 4a, the components of disp each node of the neutral surface are pı a horizontal plane. In that their dirı widely in map view, we can conclı modelled deformation is fully 3D.

Boundary effects

The lateral displacements observed on tical boundary (Fig. 4b, c) show the eı eral ramp as a geometrical boundary cı displacement values are dependent on and dip of the imposed lateral boundaı on Figure 4, and also on the thickness They document the incidence of the g lateral termination on the kinematic the basin. Moreover, we suggest that ding slip or lateral flexural-slip deforı act as evidence for a lateral terminati we could observe these features diı field.

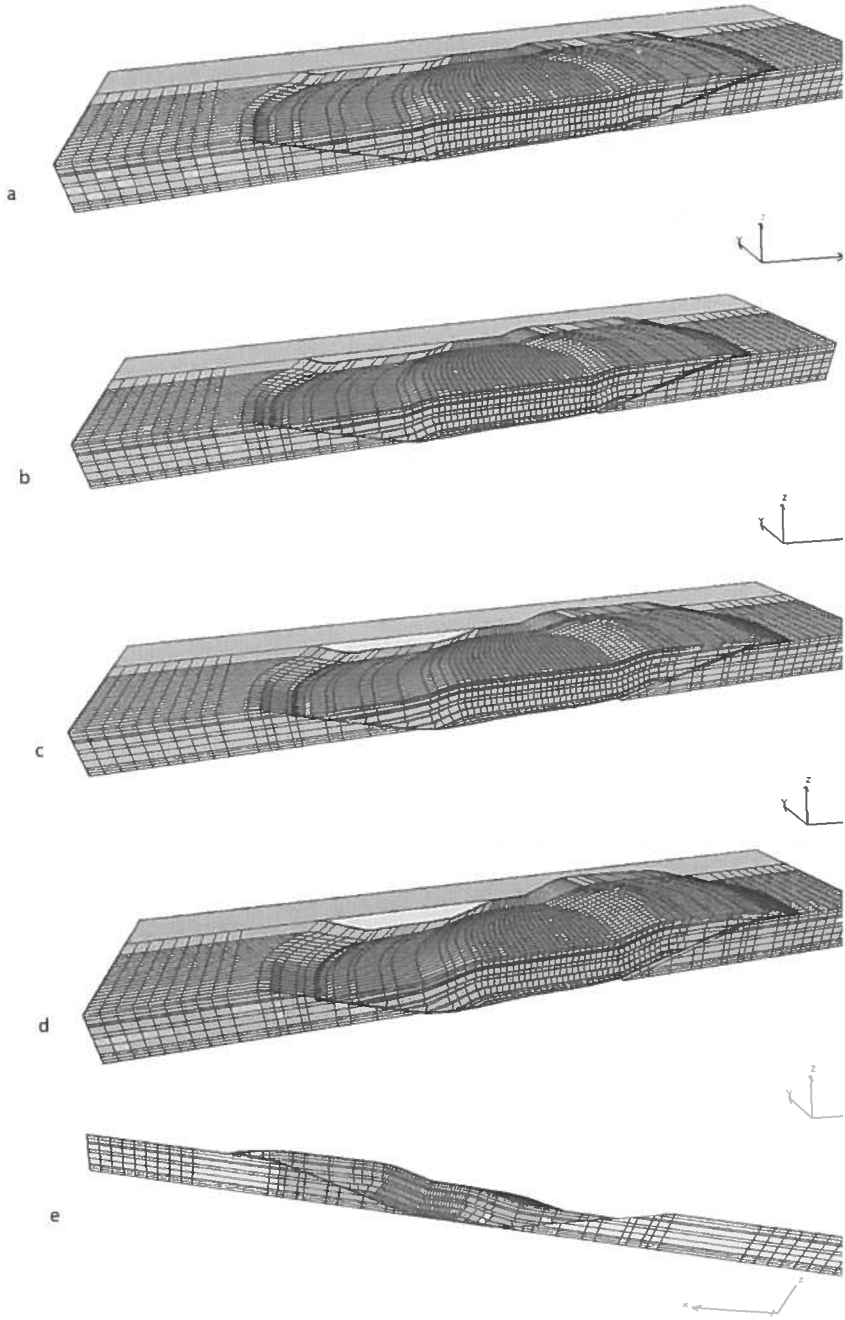

Fig. 3. (**a**) View of the deformed basin after 1000 m of displacement; (**b**) view of the deformed basi of displacement; (**c**) view of the deformed basin after 3000 m of displacement; (**d**) view of the defon 4000 m of displacement; (**e**) inverted view from the lateral imposed boundary of the deformed basi of displacement.

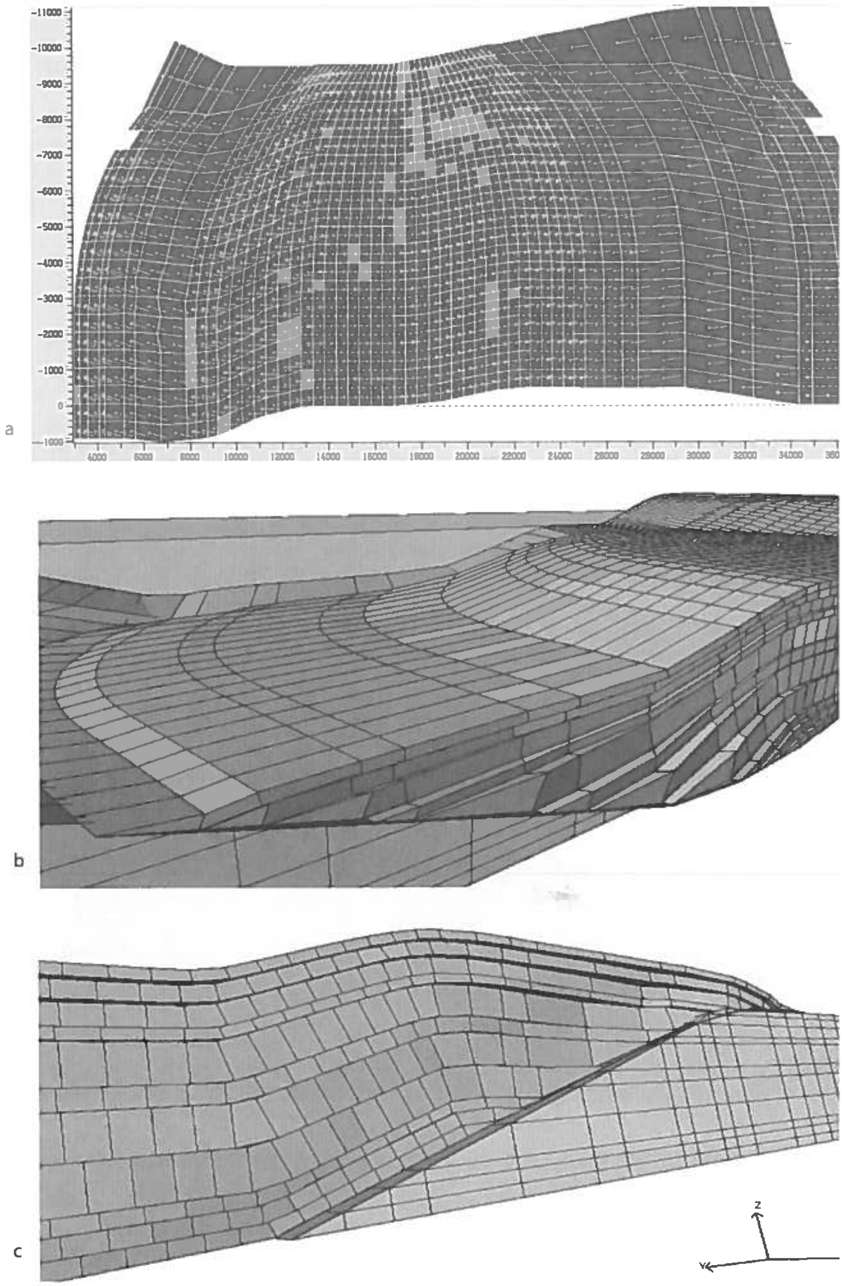

Fig. 4. (**a**) Map of the vertical projection on an horizontal plane of the neutral surface node displacemen after 4000 m of displacement; (**b**) zoom of the lateral displacements observed on the normal fault aft displacement; (**c**) zoom of the lateral displacements observed on the reverse fault after 4000 m of disp

Local volume variation

Here, the local volume variation will be designed by $\Delta V_i/V_i$, with $\Delta V_i = V_{initial} - V_{final}$. According to literature, internal strain data must usually be taken into account in 2D during balancing (V *al.* 1986; Mitra 1994; Mac Naught & but also in 3D when deformation i planar (Von Winterfeld & Oncken 1 results, the local volume variations located in particular areas (Fig. 5a–d). Volume gain is observed for elements that cross the normal fault, whereas volume loss is observed for elements that cross the reverse fault. The geometric evolution of the elements can be tied to natural processes. If $\Delta V_i/V_i$ is positive, the internal processes are responsible for a decrease of the element overlaps, with a mechanism that could relate to compaction (for example by pressure-solution (Gratier 1993), with the occurrence of stylolites in field samples). On the other hand, if $\Delta V_i/V_i$ is negative, the internal deformation increases the amount of void space between the elements, and may be matched with micro-fracturing mechanisms such as open or sealed cracks in the field. These local variations are mainly caused by the geometric properties of the geological domain: basin morphology, fault architecture, blocks or layers. For example, volume variations are broadly correlated with the thickness of the layers. However, they still remain good indicators for the localization of highly strained zones. If we look at the evolution of $\Delta V_i/V_i$ within the basin, we see that the maximal negative values are located near the hinge zone of the fault-bend folds, where the curvature of the ramp is maximum. We also see a relative attenuation of the $\Delta V_i/V_i$ when getting farther from the curvature.

Normal fault geometry

The dip of the normal fault is clearly compared with natural faults. We increased the dip of the faults; howev discrete procedure, this dip must ev ively along the entire fault in the sar listric faults. Such a complex geon tested here for simplicity.

Conclusion

The model presented here is a disc model, which offers the opportunity in extensional and compressional coupled ones. This type of modelling in order to couple tectonic deformat with the computation of fluid flow o migration during progressive deform a strong tool to study complex ge lems, even given that simplification metries may be required. It will ide better understanding of the mechani strain, and to a better representation of strain in three dimensions.

The quantitative values of the co meters, such as the local volume va

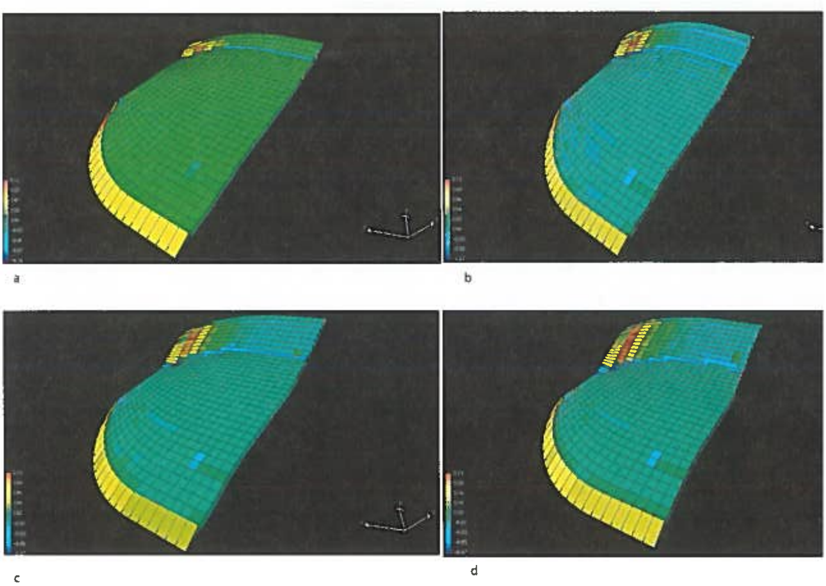

Fig. 5. The legend on the left of each picture corresponds to the $\Delta V_i/V_i$. (a) View of the local vari on the first layer after 1000 m of displacement; (b) view of the local variation of volume on the first m of displacement; (c) view of the local variation of volume on the first layer after 3000 m of displac of the local variation of volume on the first layer after 4000 m of displacement.

displacement directions, are strongly dependent on the geometry of the heterogeneous domains (faults, blocks and layers). Although the limitation of the computational scheme may restrict the numbers of layers, this is a feature common to all numerical models. Nevertheless, we believe that computed geometric and kinematic parameters should be used as semi-quantitative indicators of strain, thus allowing for comparison between 3D numerical modelling and field structures. In addition, systematic testing of the effect of the various parameters should provide general kinematic laws on the links between all these parameters, and guide further field study towards the most significant markers of the deformation (i.e. pressure-solution or fractures), both in the reservoir rock potential and seals.

References

BARNICHON, J. D. 1998. *Finite element modelling in structural and petroleum geology*. PhD thesis, Université de Liège.

BENNIS, C., VEZIEN, J. G. & IGLESIAS, G. 1991. Piecewise surface flattening for non-distorted texture mapping. *Computer Graphics,* **25(4)**, 237–246.

BOURGEOIS, E. 1997. *Mécanique des milieux poreux en tranformation finie: formulation des problèmes et méthodes de résolution*. PhD thesis, Ecole Nationale des Ponts et Chaussées.

CONTRERAS, J. & SUTER, M. 1990. Kinematic modelling of cross-sectional deformation sequences by computer simulation. *Journal of Geophysical Research,* **95**, 21 913–21 929.

CRANS, W., MANDL, G. & HAREMBOURE, J. 1980. On the theory of growth faulting: a geometrical delta model based on gravity sliding. *Journal of Petroleum Geology*, **2**, 265–307.

COUSSY, O. 1995. *Mechanics of Porous Continua*. Wiley, London.

CUNDALL, P. A. 1988. Formulation of a three-dimensional distinct element model-part I. A scheme to detect and represent contacts in a system composed of many polyhedral blocks. *International Journal of Rock Mechanics, Mineral Science & Geomechanical Abstracts,* **25(3)**, 107–116.

DAHLSTROM, C. D. A. 1969. Balanced cross sections. *Canadian Journal of Earth Sciences,* **6**, 743–757.

DE PAOR, D. G. 1988*a*. Balanced section in thrust belts, Part 1: construction. *AAPG Bulletin,* **72(1)**, 73–90.

DE PAOR, D. G. 1988*b*. Balanced section in thrust belts, Part 2: computerised line and area balancing. *Geobyte*, May, 33–37.

DIVIÈS, R. 1997. *FOLDIS: un modèle cinématique de bassins sédimentaires par éléments discrets associant plis, failles, érosion/sédimentation et compaction*. PhD thesis, Université Joseph Fourier de Grenoble.

EGAN, S. S. *et al.* 1998. Computer modelling and visualisation of the structural deformation caused by movement along geological faults. *Computers and Geosciences,* **25**, 283–297.

ERICKSON, S. G. & JAMISON, W. R. 1995. Vis finite-element models of fault-bend folds *Structural Geology,* **17**, 561–573.

GIBBS, A. D. 1983. Balanced cross-section from seismic sections in areas of extension *Journal of Structural Geology,* **5**, 153–16

GRATIER, J. P. 1993. Le fluage des roches par cristallisation sous contrainte, dans la crot *Bulletin de la société géologique de Franc* 267–287.

GRATIER, J. P. & GUILLIER, B. 1993. Compa straints on folded and faulted strata and c total displacement using computationnal (UNFOLD program). *Journal of Structur* **15(3–5)**, 391–402.

GRATIER, J. P., GUILLIER, B., DELORME, A. F. 1991. Restoration and balance of a faulted surface by best-fitting of finite ele ciples and applications. *Journal of Structu* **13(1)**, 111–115.

HART, R., CUNDALL, P. A. & LEMOS, J. 19 lation of a three dimensional distinct elen part II. Mechanical calculations for motion tion of a system composed of many polyhe *International Journal of Rock Mechani Science & Geomechanical Abstracts,* **25(3)**

MAC NAUGHT, M. A. & MITRA, G. 1996. finite strain data in constructing a retr cross-section of the Meade thrust sheet, Idaho, U.S.A. *Journal of Structural Geo* 573–583.

MITRA, G. 1994. Strain variation in thrust sl the Sevier fold-and-thrust-belt (Idaho-Utah- implications for sections restoration and evolution. *Journal of Structural Geology,* 602.

MORRETTI, I., WU, S. & BALLY, A. W. puterized balanced cross-section LOCACI struct an allochtonous salt sheet, offshore *Marine and Petroleum Geology,* **7**, 371–3

NIÑO, F., CHÉRY, J. & GRATIER, J. P. 1998. modelling of the Ventura basin : origin of t etano thrust fault and interaction with the fault. *Tectonics,* **17**, 955–972.

RAMSAY, J. G. & HUBER, M. I. 1987. *The Te Modern Structural Geology - Volume 2 : Fractures*. Academic Press, New York.

ROWAN, M. G., JACKSON, M. P. A. & TRUD 1999. Salt-related fault families and fault v northern Gulf of Mexico. *AAPG Bulletin,* 1484.

SCHNEIDER, F. & WOLF, S. 2000. Quant potentiel evaluation using 3D basin modell cation to Franklin structure, central graben, U.K. *Marine and Petroleum Geology*.

SCHNEIDER, F., WOLF, S., FAILLE, I. & PO Un modèle de bassin 3D pour l'évaluation pétrolier : application à l'offshore congola *Gas Science and Technology*.

SHAW, J. H., HOOK, S. C. & SUPPE, J. 1994 trend analysis by axial surface mapping. *etin,* **78**, 700–721.

SUPPE, J. 1983. Geometry and kinematic of folding. *American Journal of Science,* **283**, Trudgill, B. D., Rowan, M. G., Fiduk, J. C. *et al.* 1999. The perdido fold belt, Northwestern Deep Gulf of Mexico, part 1: structural geometry, evolution and regional implications. *AAPG Bulletin,* **83**, 88–113.

Von Winterfeld, C. & Oncken, O. 1995. Non-plane strain in section balancing: calculation of restoration parameters. *Journal of Structural Geology,* **17(3)**, 457–450.

Waltham, D. 1989. Finite difference modelling of hanging wall deformation. *Journal of Structural Geology,* **11**, 433–437.

Waltham, D. 1990. Finite difference modelling of sandbox analogues, compaction and detachment free deformation. *Journal of Structural Ge* 381.

Wilkerson, M. S. & Medwedeff, D. metrical modelling of fault-related f three-dimensional approach. *Journa Geology,* **13**, 801–812.

Woodward, N. B., Gray, D. R. & Spe Including strain data in balanced cross *of Structural Geology,* **8(3–4)**, 313–32

Zoetemeijer, R. 1992. *Tectonic modell basins, thin skinned thrusting, synte tation and lithospheric flexure.* PhD th ersiteit Amsterdam.